THE JOURNAL OF PHYSICAL CHEMISTRY Letters

Letter

Cite This: J. Phys. Chem. Lett. 2018, 9, 5955−5961

pubs.acs.org/JPCL

A Necessary Trade-off for Semiclassical Electrodynamics: Accurate Short-Range Coulomb Interactions versus the Enforcement of Causality?

Tao E. Li,*[,†] Hsing-Ta Chen,[†] Abraham Nitzan,[†] Maxim Sukharev,[‡,¶] and Joseph E. Subotnik*[,†]

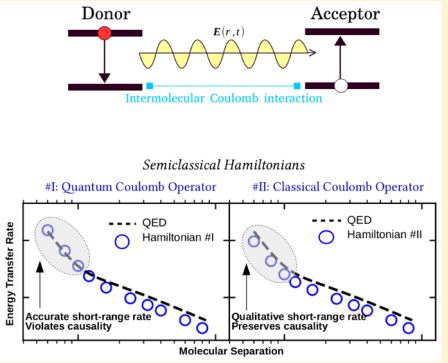
[†]Department of Chemistry, University of Pennsylvania, Philadelphia, Pennsylvania 19104, United States

[‡]Department of Physics, Arizona State University, Tempe, Arizona 85287, United States

[¶]College of Integrative Sciences and Arts, Arizona State University, Mesa, Arizona 85212, United States

Supporting Information

ABSTRACT: We investigate two key representative semiclassical approaches for propagating resonant energy transfer (RET) between a pair of electronic two-level systems (donor and acceptor) with coupled Maxwell−Liouville equations. On the one hand, when the electromagnetic (EM) field is treated classically and Coulomb interactions are treated quantum-mechanically, we find that a quantum−classical mismatch leads to a violation of causality, i.e., the acceptor can be excited before the retarded EM field arrives. On the other hand, if we invoke a classical intermolecular Coulomb operator, we find that the energy transfer in the near field loses quantitative accuracy compared with Förster theory, even though causality is strictly obeyed. Thus, our work raises a fundamental paradox when choosing a semiclassical electrodynamics algorithm. Namely, which is more important: Accurate short-range interactions or long-range causality? Apparently, one cannot have one's cake and eat it too.



Downloaded via UNIV OF PENNSYLVANIA on October 8, 2018 at 21:25:18 (UTC).
See https://pubs.acs.org/sharingguidelines for options on how to legitimately share published articles.

Light−matter interactions are an essential research area in physics, chemistry, and engineering. A host of recent experiments encountering strong light−matter interactions[1−7] have demonstrated that the optical response of matter does not always follow response theory and that we cannot always treat the electromagnetic (EM) field as a perturbation.[8−11] In order to model such experiments, an optimal approach should consider both the light and matter degrees of freedom on the same footing.

For a nonperturbative model of electrodynamics in terms of molecular properties, the usual approach is to perform a Power−Zienau−Woolley (PZW) transformation,[12,13] so that the full quantum electrodynamics (QED) Hamiltonian reads as follows

$$\hat{H} = \hat{H}_s + \frac{1}{2}\int d\mathbf{r}\left[\frac{|\hat{\mathbf{D}}_\perp(\mathbf{r})|^2}{\epsilon_0} + \frac{|\hat{\mathbf{B}}(\mathbf{r})|^2}{\mu_0}\right] - \int d\mathbf{r}\,\frac{\hat{\mathbf{D}}_\perp(\mathbf{r})}{\epsilon_0}\hat{\mathcal{P}}_\perp(\mathbf{r}) + \frac{1}{2\epsilon_0}\int d\mathbf{r}\,|\hat{\mathcal{P}}_\perp(\mathbf{r})|^2 \quad (1)$$

Here, we ignore the magnetic and diamagnetic interactions for the quantum subsystem. $\hat{\mathbf{D}}_\perp$ and $\hat{\mathbf{B}}$ are the displacement and magnetic field operators, $\hat{H}_s$ is the Hamiltonian for the quantum subsystem, and $\hat{\mathcal{P}}_\perp$ is the transverse polarization operator of the quantum (molecular) subsystem that couples to the EM field.[14] Note that the transverse component of $\hat{\mathcal{P}}$ satisfies $\nabla\cdot\hat{\mathcal{P}}_\perp = 0$, and the longitudinal component of $\hat{\mathcal{P}}$ satisfies $\nabla\times\hat{\mathcal{P}}_\parallel = 0$. $\hat{\mathbf{D}}_\perp = \epsilon_0\hat{\mathbf{E}}_\perp + \hat{\mathcal{P}}_\perp$ and $\hat{\mathbf{B}} = \nabla\times\hat{\mathbf{A}}$, where $\hat{\mathbf{A}}$ is the vector potential. The canonical commutator relationship is $[\hat{\mathbf{D}}_\perp(\mathbf{r}), \hat{\mathbf{A}}(\mathbf{r}')] = i\hbar\boldsymbol{\delta}_\perp(\mathbf{r}-\mathbf{r}')$, where $\boldsymbol{\delta}_\perp$ is the transverse δ-function. Formally, the regularized transverse δ-function can be written as $\delta_{\perp ij}(\mathbf{r}) = \frac{2}{3}\delta_{ij}\delta(\mathbf{r}) + \frac{\eta(\mathbf{r})}{4\pi r^3}\left(\frac{3r_ir_j}{r^2} - \delta_{ij}\right)$, where $i,j = x,y,z$ and $\eta(\mathbf{r}) = 0$ at $\mathbf{r} = 0$ to suppress the divergence (but $\eta(\mathbf{r}) = 1$ elsewhere).[15] Note that for a neutral system, the displacement field is exclusively transverse, (i.e., $\hat{\mathbf{D}}_\parallel = 0$), so that we can write $\hat{\mathbf{D}}$ or $\hat{\mathbf{D}}_\perp$ interchangeably. Although not discussed often, we note that eq 1 should formally include the self-interaction of all charges (which is infinitely large unless one introduces a cutoff); see eqs I.B.36 and IV.C.38 in ref 15.

At this point, let us consider a system containing N separable and neutral molecules. Here, one can write

$$\hat{H}_s = \sum_{n=1}^{N}\hat{H}_s^{(n)} + \sum_{n<l}\hat{V}_{\mathrm{Coul}}^{(nl)}$$
$$\hat{\mathcal{P}}_\perp = \sum_{n=1}^{N}\hat{\mathcal{P}}_\perp^{(n)} \quad (2)$$

Received: July 26, 2018
Accepted: September 26, 2018

© XXXX American Chemical Society

DOI: 10.1021/acs.jpclett.8b02309
J. Phys. Chem. Lett. 2018, 9, 5955−5961

where the intermolecular Coulomb interactions $\hat{V}^{(nl)}_{\mathrm{Coul}}$ are (for $n \neq l$)[15]

$$\hat{V}^{(nl)}_{\mathrm{Coul}} = \frac{1}{\epsilon_0}\int \mathrm{d}\mathbf{r}\, \hat{\boldsymbol{\mathcal{P}}}^{(n)}_{\parallel}(\mathbf{r})\cdot\hat{\boldsymbol{\mathcal{P}}}^{(l)}_{\parallel}(\mathbf{r}) \tag{3}$$

In eq 3, the intermolecular Coulomb operator is defined as the inner product of the longitudinal polarization operators for the molecules n and l. When the molecular size is much less than the intermolecular separation, one can make the point-dipole approximation, i.e., $\hat{\boldsymbol{\mathcal{P}}}^{(n)}(\mathbf{r}) = \hat{\boldsymbol{\mu}}^{(n)}\boldsymbol{\delta}(\mathbf{r}-\mathbf{r}^{(n)})$. The longitudinal polarization operator is then

$$\hat{\boldsymbol{\mathcal{P}}}^{(n)}_{\parallel}(\mathbf{r}) = \hat{\boldsymbol{\mu}}^{(n)}\boldsymbol{\delta}_{\parallel}(\mathbf{r}-\mathbf{r}^{(n)}) = \sum_{i,j}\mathbf{e}_i\left[+\frac{1}{3}\delta_{ij}\delta(\mathbf{r}-\mathbf{r}^{(n)}) - \frac{\eta(\mathbf{r}-\mathbf{r}^{(n)})}{4\pi|\mathbf{r}-\mathbf{r}^{(n)}|^3}\left(\frac{3(\mathbf{r}_i-\mathbf{r}^{(n)}_i)(\mathbf{r}_j-\mathbf{r}^{(n)}_j)}{|\mathbf{r}-\mathbf{r}^{(n)}|^2}-\delta_{ij}\right)\right]\hat{\mu}_j$$

Therefore, eq 3 can be reduced to the well-known instantaneous dipole−dipole interaction Hamiltonian[16]

$$\hat{V}^{(nl)}_{\mathrm{Coul}} = \frac{1}{4\pi\epsilon_0}\left(\frac{\hat{\boldsymbol{\mu}}^{(n)}\cdot\hat{\boldsymbol{\mu}}^{(l)}}{|\mathbf{r}|^3} - \frac{3(\hat{\boldsymbol{\mu}}^{(n)}\cdot\hat{\mathbf{r}})(\hat{\boldsymbol{\mu}}^{(l)}\cdot\hat{\mathbf{r}})}{|\mathbf{r}|^3}\right) \tag{4}$$

Here, $\hat{\boldsymbol{\mu}}^{(n,l)}$ is the dipole moment operator of molecule n or l and $\mathbf{r}$ ($\hat{\mathbf{r}}$) is the vector (unit vector) along the direction of molecular separation.

At this point, one can prove causality through the following argument. Consider the case of two molecules well separated from each other (so that $\int \mathrm{d}\mathbf{r}\, \hat{\boldsymbol{\mathcal{P}}}^{(n)}\cdot\hat{\boldsymbol{\mathcal{P}}}^{(l)} = 0$). Then, if we substitute eqs 2 and 3 into eq 1, we find that all instantaneous interactions between molecular pairs vanish by cancellation

$$\hat{H} = \sum_{n=1}^{N}\hat{H}^{(n)}_{\mathrm{s}} + \frac{1}{2}\int \mathrm{d}\mathbf{r}\left[\frac{|\hat{\mathbf{D}}_{\perp}(\mathbf{r})|^2}{\epsilon_0} + \frac{|\hat{\mathbf{B}}(\mathbf{r})|^2}{\mu_0}\right] - \sum_{n=1}^{N}\int \mathrm{d}\mathbf{r}\,\frac{\hat{\mathbf{D}}_{\perp}(\mathbf{r})}{\epsilon_0}\hat{\boldsymbol{\mathcal{P}}}^{(n)}_{\perp}(\mathbf{r}) + \sum_{n=1}^{N}\frac{1}{2\epsilon_0}\int \mathrm{d}\mathbf{r}\,|\hat{\boldsymbol{\mathcal{P}}}^{(n)}_{\perp}(\mathbf{r})|^2 \tag{5}$$

where we have used the identity

$$\begin{aligned}\hat{V}^{(nl)}_{\mathrm{Coul}} + \frac{1}{\epsilon_0}\int \mathrm{d}\mathbf{r}\,\hat{\boldsymbol{\mathcal{P}}}^{(n)}_{\perp}\cdot\hat{\boldsymbol{\mathcal{P}}}^{(l)}_{\perp} &= \frac{1}{\epsilon_0}\int \mathrm{d}\mathbf{r}\,\hat{\boldsymbol{\mathcal{P}}}^{(n)}_{\parallel}\cdot\hat{\boldsymbol{\mathcal{P}}}^{(l)}_{\parallel} + \frac{1}{\epsilon_0}\int \mathrm{d}\mathbf{r}\,\hat{\boldsymbol{\mathcal{P}}}^{(n)}_{\perp}\cdot\hat{\boldsymbol{\mathcal{P}}}^{(l)}_{\perp}\\ &= \frac{1}{\epsilon_0}\int \mathrm{d}\mathbf{r}\,\hat{\boldsymbol{\mathcal{P}}}^{(n)}\cdot\hat{\boldsymbol{\mathcal{P}}}^{(l)}\\ &= 0\end{aligned} \tag{6}$$

Thus, QED strictly satisfies causality: molecules interact solely through the retarded EM field. The Hamiltonians in eqs 1 and 5 are identical.

Semiclassical Algorithm for QED: Lack of a Unique Approach. When dealing with realistically large systems, the many-body Hamiltonians in eqs 1 and 5 are almost impossible to propagate quantum-mechanically, and the only practical method is usually time-dependent perturbation theory with small light−matter interactions. To overcome this restriction, one promising approach is to use semiclassical electrodynamics, whereby one treats the EM field classically while treating the molecular subsystem quantum mechanically and there is no small parameter.[17−21] According to this approach, one evolves the coupled Schrödinger−Maxwell or Liouville−Maxwell equations

$$\frac{\mathrm{d}}{\mathrm{d}t}\hat{\rho}(t) = -\frac{\mathrm{i}}{\hbar}[\hat{H}_{\mathrm{sc}}(t), \hat{\rho}(t)] \tag{7a}$$

$$\frac{\partial}{\partial t}\mathbf{B}(\mathbf{r}, t) = -\nabla\times\mathbf{E}(\mathbf{r}, t) \tag{7b}$$

$$\frac{\partial}{\partial t}\mathbf{E}(\mathbf{r}, t) = c^2\nabla\times\mathbf{B}(\mathbf{r}, t) - \frac{\mathbf{J}(\mathbf{r}, t)}{\epsilon_0} \tag{7c}$$

$$\mathbf{J}(\mathbf{r}, t) = \frac{\mathrm{d}}{\mathrm{d}t}\mathrm{Tr}(\hat{\rho}(t)\hat{\boldsymbol{\mathcal{P}}}(\mathbf{r})) \tag{7d}$$

Here, $\hat{\rho}$, $\hat{H}_{\mathrm{sc}}$, and $\hat{\boldsymbol{\mathcal{P}}}$ are (respectively) the density operator, the semiclassical Hamiltonian, and the polarization operator for the quantum molecular subsystem. For a subsystem containing N molecules, the total density operator $\hat{\rho}$ is expressed as $\hat{\rho} = \hat{\rho}^{(1)}\otimes\hat{\rho}^{(2)}\otimes\cdots\otimes\hat{\rho}^{(N)}$. In eq 7c, $c = 1/\sqrt{\mu_0\epsilon_0}$ and $\mathbf{J}$ is the current density operator that connects the quantum molecular subsystem to the classical EM field. In eq 7d, $\mathbf{J}$ is defined by a mean-field approximation,[22,23] and therefore eq 7 can also be called "'Ehrenfest'" electrodynamics. As far as the notation below, it will be crucial to distinguish between the operator $\hat{\boldsymbol{\mathcal{P}}}$ (with a hat) and the average $\boldsymbol{\mathcal{P}} = \mathrm{Tr}(\hat{\rho}\hat{\boldsymbol{\mathcal{P}}})$ (no hat).

Note that eq 7c can be separated into two different equations for the transverse and perpendicular components

$$\frac{\partial}{\partial t}\mathbf{E}_{\perp}(\mathbf{r}, t) = c^2\nabla\times\mathbf{B}(\mathbf{r}, t) - \frac{\mathbf{J}_{\perp}(\mathbf{r}, t)}{\epsilon_0} \tag{8a}$$

$$\frac{\partial}{\partial t}\mathbf{E}_{\parallel}(\mathbf{r}, t) = -\frac{\mathbf{J}_{\parallel}(\mathbf{r}, t)}{\epsilon_0} \tag{8b}$$

and the latter equation can be integrated so that

$$\mathbf{E}_{\parallel}(\mathbf{r}, t) = -\frac{\boldsymbol{\mathcal{P}}_{\parallel}(\mathbf{r}, t)}{\epsilon_0} \tag{9}$$

Hamiltonian #I. When defining the semiclassical, electronic Hamiltonian $\hat{H}_{\mathrm{sc}}$ in eq 7a, there is no unique prescription. In the Supporting Information, we provide a detailed approach for constructing two different semiclassical Hamiltonians starting from the PZW Hamiltonian. Here, we present only the main results.

The first Hamiltonian[13] reads

$$\hat{H}^{\mathrm{I}}_{\mathrm{sc}} = \sum_{n=1}^{N}\left[\hat{H}^{(n)}_{\mathrm{s}} - \int \mathrm{d}\mathbf{r}\,\mathbf{E}_{\perp}(\mathbf{r}, t)\cdot\hat{\boldsymbol{\mathcal{P}}}^{(n)}(\mathbf{r})\right] + \sum_{n<l}\hat{V}^{(nl)}_{\mathrm{Coul}} \tag{10}$$

Henceforward, we will refer to eq 10 as Hamiltonian #I.

In eq 10, there are two terms containing instantaneous interactions: the nonlocal transverse E-field ($\mathbf{E}_{\perp}$) and the intermolecular Coulomb interactions ($\hat{V}^{(nl)}_{\mathrm{Coul}}$). Just as for QED, one would normally expect that eqs 7−10 should preserve causality. This alleged cancellation should be obvious if we

DOI: 10.1021/acs.jpclett.8b02309
J. Phys. Chem. Lett. 2018, 9, 5955−5961

substitute in $\mathbf{E}_\perp = \mathbf{E} - \mathbf{E}_\parallel = \mathbf{E} + \frac{1}{\epsilon_0}\boldsymbol{\mathcal{P}}_\parallel$, so that we can rewrite eq 10 as

$$\hat{H}_{sc}^{I} = \sum_{n=1}^{N}\left[\hat{H}_s^{(n)} - \int d\mathbf{r}\left(\mathbf{E}(\mathbf{r},t) + \frac{1}{\epsilon_0}\boldsymbol{\mathcal{P}}_\parallel^{(n)}(\mathbf{r})\right)\cdot\hat{\boldsymbol{\mathcal{P}}}^{(n)}(\mathbf{r})\right] - \frac{1}{\epsilon_0}\sum_{n\neq l}\int d\mathbf{r}\,\boldsymbol{\mathcal{P}}_\parallel^{(n)}(\mathbf{r})\cdot\hat{\boldsymbol{\mathcal{P}}}^{(l)}(\mathbf{r}) + \sum_{n<l}\hat{V}_{Coul}^{(nl)} \tag{11}$$

Ideally, the second line of eq 11 should cancel (see eq 6). However, note that in eq 11 one of the $\boldsymbol{\mathcal{P}}$ terms is treated classically while the Coulomb interactions are treated fully quantum-mechanically (see eq 3), and thus, there is no guarantee of cancellation or strict causality. In fact, below we will present numerical simulations showing that causality is not strictly enforced. Thus, one may further ask, can we find a different semiclassical Hamiltonian that does preserve causality? Indeed, this is possible, which brings us to Hamiltonian #II.

Hamiltonian #II. To preserve causality, one can make the following approximation: $\forall n,l$,

$$\hat{V}_{Coul}^{(nl)} = \frac{1}{\epsilon_0}\int d\mathbf{r}\,\boldsymbol{\mathcal{P}}_\parallel^{(n)}(\mathbf{r},t)\cdot\hat{\boldsymbol{\mathcal{P}}}_\parallel^{(l)}(\mathbf{r}) + \frac{1}{\epsilon_0}\int d\mathbf{r}\,\boldsymbol{\mathcal{P}}_\parallel^{(l)}(\mathbf{r},t)\cdot\hat{\boldsymbol{\mathcal{P}}}_\parallel^{(n)}(\mathbf{r}) \tag{12}$$

Compared with the quantum form of $\hat{V}_{Coul}^{(nl)}$ in eq 3, the physical meaning of eq 12 is clear: the intermolecular Coulomb interactions between molecules are effectively the classical polarization energies as felt by one molecule in the field of another and as expressed by the classical longitudinal polarization fields ($\boldsymbol{\mathcal{P}}_\parallel^{(n)}$ and $\boldsymbol{\mathcal{P}}_\parallel^{(l)}$). If we substitute eq 12 and $\mathbf{E}_\perp = \frac{1}{\epsilon_0}(\mathbf{D} - \boldsymbol{\mathcal{P}}_\perp)$ into eq 10, after some straightforward algebra, we find that a new semiclassical Hamiltonian emerges

$$\hat{H}_{sc}^{II} = \sum_{n=1}^{N}\hat{H}_s^{(n)} - \frac{1}{\epsilon_0}\int d\mathbf{r}\,\mathbf{D}(\mathbf{r},t)\cdot\hat{\boldsymbol{\mathcal{P}}}^{(n)}(\mathbf{r}) + \frac{1}{\epsilon_0}\int d\mathbf{r}\,\boldsymbol{\mathcal{P}}_\perp^{(n)}(\mathbf{r},t)\cdot\hat{\boldsymbol{\mathcal{P}}}^{(n)}(\mathbf{r}) \tag{13}$$

In eq 13, the intermolecular interactions are carried exclusively through the classical D-field, and thus, causality is strictly preserved. Henceforward, to distinguish eq 13 from eq 10, we will refer to eq 13 as Hamiltonian #II. Note that by substituting eq 12 into eq 11, eq 13 is equivalent to

$$\hat{H}_{sc}^{II} = \sum_{n=1}^{N}\left[\hat{H}_s^{(n)} - \int d\mathbf{r}\left(\mathbf{E}(\mathbf{r},t) + \frac{1}{\epsilon_0}\boldsymbol{\mathcal{P}}_\parallel^{(n)}(\mathbf{r})\right)\cdot\hat{\boldsymbol{\mathcal{P}}}^{(n)}(\mathbf{r})\right] \tag{14}$$

Hamiltonians #I′/#II′. Before presenting any results, one final point is appropriate. As discussed above, eq 1 should formally include the self-interaction of all charges. Also, for a single electron at each site n, this self-interaction will be of the form $\hat{V}_{self} = \frac{1}{2\epsilon_0}\int d\mathbf{r}\,|\hat{\boldsymbol{\mathcal{P}}}_\parallel^{(n)}|^2$. If we make a semiclassical approximation (in the spirit of eqs 3 and 12), we can approximate $\hat{V}_{self} = \frac{1}{\epsilon_0}\int d\mathbf{r}\,\boldsymbol{\mathcal{P}}_\parallel^{(n)}\cdot\hat{\boldsymbol{\mathcal{P}}}_\parallel^{(n)}$, which will obviously cancel the self-interaction terms in eqs 11 and 14. The resulting Hamiltonians will be of the form

$$\hat{H}_{sc}^{I'} = \sum_{n=1}^{N}\left[\hat{H}_s^{(n)} - \int d\mathbf{r}\,\mathbf{E}(\mathbf{r},t)\cdot\hat{\boldsymbol{\mathcal{P}}}^{(n)}(\mathbf{r})\right] - \frac{1}{\epsilon_0}\sum_{n\neq l}\int d\mathbf{r}\,\boldsymbol{\mathcal{P}}_\parallel^{(n)}(\mathbf{r})\cdot\hat{\boldsymbol{\mathcal{P}}}^{(l)}(\mathbf{r}) + \sum_{n<l}\hat{V}_{Coul}^{(nl)} \tag{15a}$$

$$\hat{H}_{sc}^{II'} = \sum_{n=1}^{N}\hat{H}_s^{(n)} - \int d\mathbf{r}\,\mathbf{E}(\mathbf{r},t)\cdot\hat{\boldsymbol{\mathcal{P}}}^{(n)}(\mathbf{r}) \tag{15b}$$

In practice, as shown in the Supporting Information, we find that $\hat{H}_{sc}^{I'}$ and $\hat{H}_{sc}^{II'}$ behave effectively the same as $\hat{H}_{sc}^{I}$ and $\hat{H}_{sc}^{II}$. In the Supporting Information, we list the relevant energy expression that is conserved for each choice of $\hat{H}_{sc}$.

Comparison of the Different Hamiltonians. When comparing Hamiltonians #I and #II, it is very important to emphasize that, although we have derived $\hat{H}_{sc}^{II}$ by invoking the approximation in eq 12, $\hat{H}_{sc}^{II}$ can also be derived directly from the PZW Hamiltonian. $\hat{H}_{sc}^{II}$ should not be considered any less valid than $\hat{H}_{sc}^{I}$; see the Supporting Information.

Next, let us comment on the issues of electronic correlation and quantum entanglement. As far as quantum entanglement is concerned, with semiclassical electrodynamics, there cannot be any strict quantum entanglement between electrons and photons because the EM field is treated classically. Nevertheless, even with Ehrenfest dynamics, there is some feedback from the electronic degrees of freedom to the photon field, and there is certainly some correlation between the boson field and the electronic state at any given time.[24] A great deal of research has now shown that Ehrenfest equations of motion can sometimes yield the proper dynamics for Fermionic subsystems coupled to bosonic baths (especially provided that one works with the correct initial conditions).[25,26]

Let us now move our attention to electron−electron correlation. One the one hand, because Hamiltonian #I contains a quantum two-body operator (i.e., $\hat{V}_{Coul}^{(nl)}$ in eqs 3 and 4), this method allows for entanglement between individual molecules. On the other hand, by invoking a classical intermolecular Coulomb operator in eq 12, Hamiltonian #II does not allow for entanglement between molecules. As a practical matter, in what follows below, we will see that these differences can lead to different energy transfer rates.

To compare the two semiclassical Hamiltonians above, we will now apply Ehrenfest electrodynamics and model resonant energy transfer (RET) between a pair of identical electronic two-level systems (TLSs)[27−30] in three dimensions.

Model. Consider a pair of TLSs with a donor (D) and an acceptor (A). The Hamiltonian for both the donor and acceptor are

$$\hat{H}_s^{(D)} = \hat{H}_s^{(A)} = \begin{pmatrix} 0 & 0 \\ 0 & \hbar\omega_0 \end{pmatrix} \tag{16}$$

where eq 16 is expressed in the basis $\{|g\rangle,|e\rangle\}$; here $|g\rangle$ is the ground state and $|e\rangle$ is the excited state. $\hbar\omega_0$ is the energy difference between $|g\rangle$ and $|e\rangle$. The polarization operator for each molecule reads

$$\hat{\boldsymbol{\mathcal{P}}}^{(n)}(\mathbf{r}) = \boldsymbol{\xi}(\mathbf{r} - \mathbf{r}_0^{(n)})\begin{pmatrix} 0 & 1 \\ 1 & 0 \end{pmatrix} \qquad n = D, A \tag{17}$$

Here, $\boldsymbol{\xi}(\mathbf{r}) = \psi_g^* q\mathbf{r}\psi_e = (2\pi)^{-3/2}\sigma^{-5}\mu_{12}\mathbf{r}z\exp(-r^2/2\sigma^2)$ is the polarization density of a TLS where $|g\rangle$ is an s-orbital, $|e\rangle$ is a p_z orbital, q denotes the effective charge of the TLS, σ denotes

DOI: 10.1021/acs.jpclett.8b02309
J. Phys. Chem. Lett. 2018, 9, 5955−5961

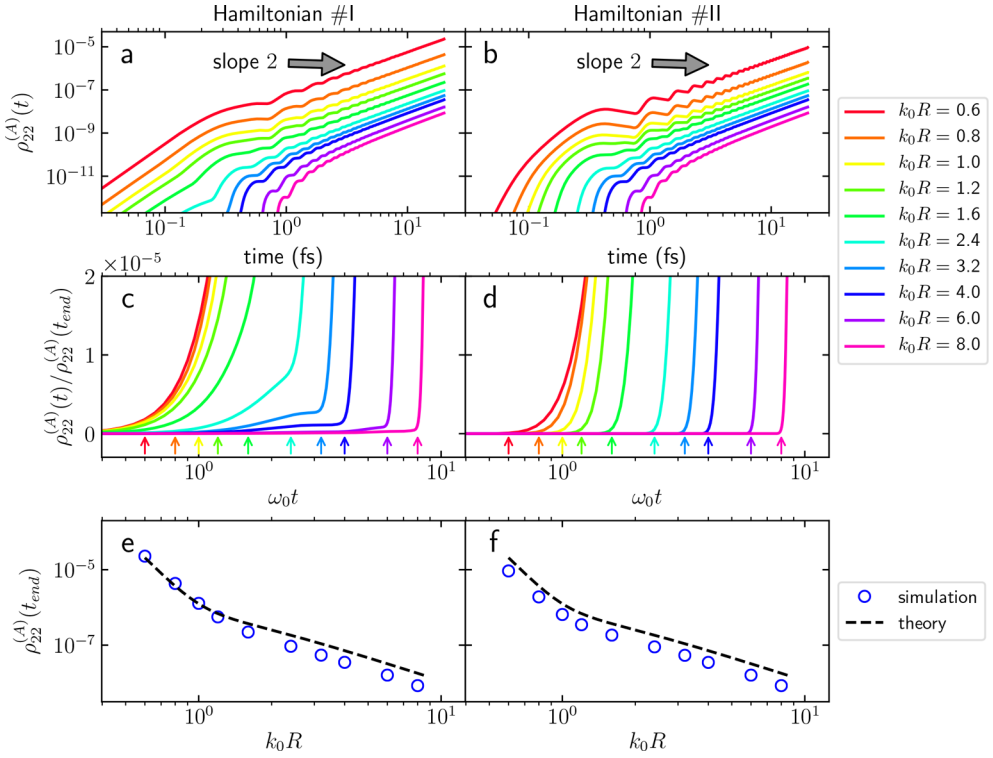


Figure 1. Plot of the excited state population of the acceptor ($\rho_{22}^{(A)}(t)$) at short times (t_{end} = 20 fs). Results for Hamiltonian #I (II) are plotted on the left (right). (a,b) $\rho_{22}^{(A)}(t)$ versus time using a logarithmic scale by varying the separation in the range $0.6 \leq k_0R \leq 8.0$ (rainbow color from red to purple, respectively), where $k_0 = \omega_0/c$. (c,d) Normalized $\rho_{22}^{(A)}$ ($\rho_{22}^{(A)}(t)/\rho_{22}^{(A)}(t_{\mathrm{end}})$) versus $\omega_0 t$ with the same separation range as that in panels (a) and (b), where now only the x-axis is plotted logarithmically. (e,f) $\rho_{22}^{(A)}(t_{\mathrm{end}})$ versus k_0R on a logarithmic scale; the simulation data (blue circles) of Hamiltonians #I and #II are compared with the QED result (eq 20, black dashed line). The initial state for the donor is $(C_1^{(D)}(0), C_2^{(D)}(0)) = (1/\sqrt{2}, 1/\sqrt{2})$ and the initial state for the acceptor is $(C_1^{(A)}(0), C_2^{(A)}(0)) = (1, 0)$. Other parameters are given in the Supporting Information. Note that in panels (a) and (b), the straight lines when $t > 2$ fs indicate that the leading term of $\rho_{22}^{(A)}(t)$ varies as $\sim t^2$ (the same as eq 20). Note that Hamiltonian #I (c) violates causality such that $\rho_{22}^{(A)}(t) > 0$ before the retarded field from the donor comes ($\omega_0 t < k_0 R$), while Hamiltonian #II (d) exactly preserves causality; see the rainbow arrows indicating the time before which energy transfer is not allowed by causality. In panels (e) and (f), both Hamiltonians show R^{-6} dependence when $k_0R < 1$ and R^{-2} dependence when $k_0R > 1$. However, Hamiltonian #I agrees with QED better for short separations than Hamiltonian #II, presumably because the former describes Coulomb interactions quantum-mechanically.

the width of wave functions, and $\mu_{12} = |\int \mathrm{d}\mathbf{r}\, \psi_g^* q\mathbf{r}\psi_e|$ denotes the magnitude of the transition dipole moment. We assume that the TLS has no permanent dipole. Without loss of generality, we suppose that the donor (acceptor) sits on the negative (positive) side of the x-axis, i.e., $\mathbf{r}_0^{(D)} = (-R/2,0,0)$ and $\mathbf{r}_0^{(A)} = (R/2,0,0)$. We define R as the separation between the two TLSs.

Overall, the electronic Hamiltonians read as follows in matrix form (in the basis $\{|gg\rangle, |ge\rangle, |eg\rangle, |ee\rangle\}$)

$$\hat{H}_{\mathrm{sc}}^{\mathrm{I}} = \begin{pmatrix} 0 & \nu_A & \nu_D & \nu \\ \nu_A & \hbar\omega_0 & \nu & \nu_D \\ \nu_D & \nu & \hbar\omega_0 & \nu_A \\ \nu & \nu_D & \nu_A & 2\hbar\omega_0 \end{pmatrix} \tag{18}$$

and

$$\hat{H}_{\mathrm{sc}}^{\mathrm{II}} = \begin{pmatrix} 0 & \nu_A' & \nu_D' & 0 \\ \nu_A' & \hbar\omega_0 & 0 & \nu_D' \\ \nu_D' & 0 & \hbar\omega_0 & \nu_A' \\ 0 & \nu_D' & \nu_A' & 2\hbar\omega_0 \end{pmatrix} \tag{19}$$

where $\nu = \frac{1}{\epsilon_0}\int \mathrm{d}\mathbf{r}\, \boldsymbol{\xi}_{\parallel}^{(D)} \cdot \boldsymbol{\xi}_{\parallel}^{(A)}$, $\nu_D = -\int \mathrm{d}\mathbf{r}\, \mathbf{E}_{\perp} \cdot \boldsymbol{\xi}^{(D)}$ and $\nu_D' = -\frac{1}{\epsilon_0}\int \mathrm{d}\mathbf{r}\, \boldsymbol{\xi}^{(D)} \cdot (\mathbf{D} - 2\mathrm{Re}\, \rho_{12}^{(D)} \boldsymbol{\xi}_{\perp}^{(D)})$, and ν_A and ν_A' are defined analogously. All other simulation details and parameters are provided in the Supporting Information.

Analytical QED Results. When modeling RET with retardation,[31−33] it is well-known that energy transfer rates show an R^{-6} dependence when $k_0R \ll 1$ and an R^{-2} dependence when $k_0R \gg 1$. Here $k_0 \equiv \omega_0/c$. This difference in scaling arises because the usual instantaneous version of energy transfer theory[34−36] does not account for the dynamical motion of the EM field to carry energy from the donor to acceptor. For our purposes, in order to directly compare with simulation, we will require an accurate calculation of energy transfer dynamics (beyond any rate expression, e.g., Förster theory) that is exact within QED perturbation theory. A short-time analytical formula of the excited state population of the acceptor, $\rho_{22}^{(A)}(t)$, can be derived with QED, as shown by Power, Thirunamachandran, and Salam.[37,38] By slightly modifying the result in ref 38, we can obtain an analytical solution for $\rho_{22}^{(A)}(t)$ at short times, starting in an arbitrary superposition state for the donor (see the Supporting Information)

DOI: 10.1021/acs.jpclett.8b02309
J. Phys. Chem. Lett. 2018, 9, 5955−5961

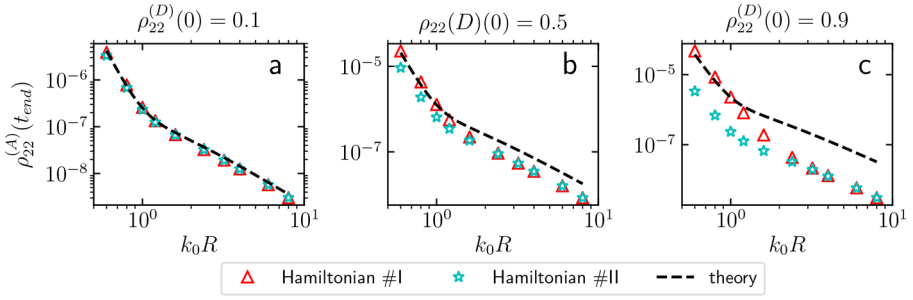


Figure 2. Plot of the excited state population of the acceptor at the end time ($\rho_{22}^{(A)}(t_{end}$; t_{end} = 20 fs) versus the intermolecular separation (k_0R) using a logarithmic scale. Simulations are performed with different initial excited state populations for the donor: $\rho_{22}^{(D)}(0)$ = 0.1 (left), 0.5 (middle), and 0.9 (right). Three methods are compared: Hamiltonian #I (red triangle), Hamiltonian #II (cyan star), and QED (eq 20, black dashed line). Parameters are given in the Supporting Information. Note that when $\rho_{22}^{(D)}(0)$ is small, all methods agree with each other. As $\rho_{22}^{(D)}(0)$ increases, there is less agreement between Hamiltonians #I/II and the QED result. Just as for Figure 1, due to its quantum-mechanical description of Coulomb interactions, Hamiltonian #I always agrees with QED better for short separations (unlike Hamiltonian #II).

$$\rho_{22}^{(A)}(t) = \frac{\rho_{22}^{(D)}(0)}{(4\pi\epsilon_0\hbar)^2}\left|\mu_{12}^{D}\mu_{12}^{A}\left[-\eta_1\frac{k_0^{\,2}}{R} + \eta_3\left(\frac{1}{R^3} - \frac{ik_0}{R^2}\right)\right]\right|^2 \times \left(t - \frac{R}{c}\right)^2\theta\left(t - \frac{R}{c}\right) \tag{20}$$

Here, $\rho_{22}^{(D)}(0)$ is the initial excited state population of the donor, $\mathbf{e}_D$ and $\mathbf{e}_A$ are the unit vectors oriented along the transition dipoles of the donor and the acceptor, $\eta_1 = \mathbf{e}_A \cdot \mathbf{e}_D - (\mathbf{e}_A \cdot \mathbf{e}_R)(\mathbf{e}_D \cdot \mathbf{e}_R)$, and $\eta_3 = \mathbf{e}_A \cdot \mathbf{e}_D - 3(\mathbf{e}_A \cdot \mathbf{e}_R)(\mathbf{e}_D \cdot \mathbf{e}_R)$. We define $\mathbf{e}_R$ as the unit vector oriented along the separation between the donor and acceptor. In our model, the pair of TLSs is located along the x-axis, and the transition dipole moments are both p_z polarized, so that $\mathbf{e}_A \cdot \mathbf{e}_R = \mathbf{e}_D \cdot \mathbf{e}_R = 0$ and $\eta_1 = \eta_3 = \mathbf{e}_A \cdot \mathbf{e}_D = 1$. $\theta(t) = \frac{d}{dt}\mathrm{Max}\{t, 0\}$ is the Heaviside step function.

Note that the unretarded energy transfer expression for $\rho_{22}^{(A)}$ is simply $\rho_{22}^{(A)}(t) = \rho_{22}^{(D)}(0) \times \frac{|\mu_{12}^{D}|^2|\mu_{12}^{A}|^2}{(4\pi\epsilon_0\hbar)^2R^6}\eta_3^{\,2}t^2$, which is equivalent to the FGR result with the coupling $\hat{V}_{\mathrm{Coul}}^{(nl)}$ in eq 4. Equation 20 includes two important time-dependent features: (i) all retardation is totally accounted for (i.e., $\rho_{22}^{(A)}(t)$ is zero when $t < R/c$) and (ii) $\rho_{22}^{(A)}(t)$ depends quadratically on time at short times.

Numerical Semiclassical Results. As far as simulating energy transfer semiclassically, we will assume that there is no EM field in space initially; the donor starts in a superposition state $(C_1^{(D)}(0), C_2^{(D)}(0)) = (1/\sqrt{2}, 1/\sqrt{2})$, and the acceptor starts in the ground state, where C_1 (C_2) represents the quantum amplitude of $|g\rangle$ ($|e\rangle$). With these initial conditions, we can propagate eq 7 and compare dynamics of Hamiltonians #I and #II. To keep the following context concise, we will refer to the result of Hamiltonian #I (II) as result #I (II) for short.

In Figure 1, we plot the excited state population of the acceptor ($\rho_{22}^{(A)}(t)$) at relatively short times (t < 20 fs) by varying the separation R ($0.6 \leq k_0R \leq 8.0$). In Figure 1c, we find that result #I clearly does not preserve causality: $\rho_{22}^{(A)}(t)$ begins to increase even before the retarded field from the donor arrives ($\omega_0 t < k_0R$); see the Supporting Information for a discussion of causality. Interestingly, however, for very large distances (when $k_0R \gg 1$), Hamiltonian #I seems to do a better job of preserving causality because, in this limit, the intermolecular interactions are dominated by the retarded field (which decays as R^{-1}) rather than longitudinal Coulomb interactions (which decay as R^{-3}). Nevertheless, clearly, Hamiltonian #I violates the tenets of relativity. That being said, Hamiltonian #II does preserve causality exactly (see Figure 1d). Thus, from this perspective, one would presume that Hamiltonian #II has an obvious advantage over Hamiltonian #I.

At this point, however, let us turn our attention to Figure 1e,f. Here, we compare rates of energy transfer for the two methods as compared with the analytic theory in eq 20 as a function of R. According to Figure 1e,f, even though results #I and #II (blue circles) recover qualitatively the same distance dependencies as those for eq 20 (black lines), results #I and #II differ in the limit of short donor−acceptor separation (k_0R < 1). For short distances, result #I agrees exactly with QED (eq 20), while result #II is off by roughly a factor of 2. This discrepancy is perhaps not surprising because at short separation the dominant Coulomb interactions are described quantum-mechanically in Hamiltonian #I but are classical in Hamiltonian #II, and there is no reason to suppose that these two methods should agree quantitatively in practice. By contrast, at long separations (k_0R > 1), where the retarded field is dominant, both Hamiltonians #I and #II propagate the retarded field classically, and therefore, both methods should agree; interestingly, in this limit, both semiclassical approaches differ from the QED results by roughly a factor of 2.[39]

Can We Model Energy Transfer Accurately without Spontaneous Emission? At large separation ($k_0R \gg 1$), it is clear that RET is dominated by the dynamics of the radiation field: retardation effects appear and the RET rate scales as $1/R^2$ instead of the usual $1/R^6$ scaling (i.e., the Förster scaling that arises from the instantaneous dipole−dipole interactions). Now, for this reason, if semiclassical theory is to model RET correctly, it is clear that one must treat spontaneous emission correctly. After all, at long distances, RET can effectively be considered as the result of spontaneous emission from the donor, followed subsequently by absorption of the acceptor. That being said, however, we must emphasize that Ehrenfest electrodynamics do not recover the full FGR spontaneous emission rate.[21,40,41] Instead, as shown in ref 21, Ehrenfest dynamics predict a decay rate (k_{Eh}) proportional to the instantaneous ground state population

$$k_{\mathrm{Eh}}(t) = \rho_{11}(t)k_{\mathrm{FGR}} \tag{21}$$

One can argue that this failure arises from the fact that Ehrenfest electrodynamics predict only a coherent scattering

DOI: 10.1021/acs.jpclett.8b02309
J. Phys. Chem. Lett. 2018, 9, 5955−5961

field (which is proportional to the ground state population of the molecule) without any incoherent scattering.[42,43] In other words, according to a single Ehrenfest trajectory, one would predict $\langle\hat{\mathbf{E}}\rangle^2 = \langle\hat{\mathbf{E}}^2\rangle$, which is not correct quantum-mechanically. By contrast, according to quantum treatment, both coherent and incoherent scattering are allowed, and interference effects can lead to situations where, in the extreme case, $\langle\hat{\mathbf{E}}\rangle = 0$ but $\langle\hat{\mathbf{E}}\rangle^2 \neq 0$, as is common for spontaneous emission. Thus, to sum up, modeling RET robustly requires more than a single classical ansatz for the electric field at one time, $\langle\hat{\mathbf{E}}(t)\rangle$: a FGR calculation relies on capturing the correct time correlation function for the electric field, $\langle\hat{\mathbf{E}}(0)\hat{\mathbf{E}}(t)\rangle$; see the note about averaging Ehrenfest trajectories in the Supporting Information.

With this background and eq 21 in mind, one might expect that the Ehrenfest energy transfer rate would depend strongly on the initial state population, and one can ask, will our results using Hamiltonians #I and #II change in a similar fashion for different initial states? To that end, in Figure 2, for a variety of initial conditions, we compare results for $\rho_{22}^{(A)}(t)$ as calculated according to both Hamiltonians #I (red triangle) and #II (cyan star). We also plot the short-time full QED results (black dashed line) from eq 20, where the initial excited state population is reflected in the initial donor ($\rho_{22}^{(D)}(0)$).

Our results are plotted in Figure 2. When the donor is weakly excited initially ($\rho_{22}^{(D)}(0) = 0.1$), we find that all three results agree with each other. However, when $\rho_{22}^{(D)}(0)$ is increased, we find less and less agreement between either of the semiclassical results and QED results at long distances; the semiclassical results strongly underestimate the energy transfer rate. These results strongly suggest that if a semiclassical approach is to capture energy transfer accurately both at short and long distances, the approach must be able to capture spontaneous emission as well. After all, at long distances, we know that energy transfer is modulated by a retarded field, and if Ehrenfest dynamics cannot capture spontaneous emission, there is no surprise that one cannot recover the correct energy transfer rate either.

Lastly, let us now consider results at short distances. Here, we find very different behavior between Hamiltonians #I and #II. On the one hand, we find that, no matter the initial donor population, Hamiltonian #I always produces accurate results; because Hamiltonian #I includes explicitly quantum-mechanical Coulomb interactions, we believe that this method should always agree with QED at short-range (where retardation effects are not important). On the other hand, in Figure 2c, we also see that Hamiltonian #II fails and drastically underestimates the energy transfer rate for $\rho_{22}^{(D)}(0) = 0.9$. Here, we need only recognize that because Hamiltonian #II treats the EM field exclusively classically, such an approach can never be accurate (either at short-range or at long-range) if spontaneous emission is not capture correctly. Thus, in the end, a crucial question emerges: If we can develop a means to include spontaneous emission on top of Ehrenfest dynamics (as in ref 43), what will be the most accurate approach: to include a combination of quantum Coulomb interactions with a classical (but exclusively transverse) EM field (i.e., Hamiltonian #I) or to employ an entirely classical (transverse plus longitudinal) EM field? The answer is not obvious, especially because the full nature of a quantum radiation field cannot be captured by simply including spontaneous emission. Hence, a thorough benchmark will be necessary. As we look forward to future methodological development of this understudied area, many questions remain.

In conclusion, by numerically studying coherent energy transfer between a pair of TLSs with Ehrenfest electrodynamics, our conclusions are as follows: (i) The standard Hamiltonian #I ($\hat{H}_{sc}^{I}$ in eq 10) violates causality, especially when the molecular separation is small ($k_0R < 1$) because of a mismatch between a *quantum* description of the matter and a *classical* description of the EM field; (ii) causality can be preserved if one models both the retarded field and the intermolecular Coulomb interactions in a classical fashion (Hamiltonian $\hat{H}_{sc}^{II}$ in eq 13); (iii) for RET, both Hamiltonians #I and #II predict qualitatively the same distance behavior as retarded Förster theory, and when the electronic excitation of the donor is weak, both semiclassical methods recover QED results quantitatively; however, (iv) even though Hamiltonian #I violates causality, this approach better agrees with QED with regards to RET rates at short distances. The pros and cons of these different Hamiltonians suggest that the specific choice of a semiclassical Hamiltonian may depend on the particular problem that one is investigating; for now, it would appear that there is no sinecure for the inconsistencies inevitably faced by a semiclassical ansatz. Nevertheless, if spontaneous emission can be incorporated into Ehrenfest dynamics, the accuracy of these methods should be dramatically enhanced. This work is ongoing in our laboratory.

■ ASSOCIATED CONTENT

Supporting Information

The Supporting Information is available free of charge on the ACS Publications website at DOI: 10.1021/acs.jpclett.8b02309.

Derivation of semiclassical Hamiltonians; simulation details and parameters; the conserved quantity for each semiclassical Hamiltonian discussed; results for Hamiltonians #I′ and #II′, showing that self-interaction is not important for accurately modeling the dynamics of energy transfer; details regarding the derivation of eq 20 and a comment on applying Weisskopf–Wigner theory to RET; a brief discussion of causality in Figure 1; and a more detailed explanation for why we must average over many Ehrenfest trajectories (rather than a single trajectory) (PDF)

■ AUTHOR INFORMATION

Corresponding Authors

*E-mail: taoli@sas.upenn.edu (T.E.L.).
*E-mail: subotnik@sas.upenn.edu (J.E.S.).

ORCID

Tao E. Li: 0000-0003-0361-5687
Abraham Nitzan: 0000-0002-8431-0967

Notes

The authors declare no competing financial interest.

■ ACKNOWLEDGMENTS

This material is based upon work supported by the National Science Foundation under Grant No. CHE-1764365 (T.L., H.T.C., J.E.S.), AFOSR Grant No. FA9550-15-1-0189 (M.S.), U.S.–Israel Binational Science Foundation Grant No. 2014113 (M.S. and A.N.), and the U.S. National Science Foundation Grant No. CHE1665291 (A.N.).

DOI: 10.1021/acs.jpclett.8b02309
J. Phys. Chem. Lett. 2018, 9, 5955–5961

REFERENCES

(1) Törmä, P.; Barnes, W. L. Strong Coupling Between Surface Plasmon Polaritons and Emitters: a Review. *Rep. Prog. Phys.* **2015**, *78*, 013901.

(2) Sukharev, M.; Nitzan, A. Optics of Exciton-plasmon Nanomaterials. *J. Phys.: Condens. Matter* **2017**, *29*, 443003.

(3) Vasa, P.; Lienau, C. Strong Light−Matter Interaction in Quantum Emitter/Metal Hybrid Nanostructures. *ACS Photonics* **2018**, *5*, 2−23.

(4) Khitrova, G.; Gibbs, H. M.; Kira, M.; Koch, S. W.; Scherer, A. Vacuum Rabi Splitting in Semiconductors. *Nat. Phys.* **2006**, *2*, 81−90.

(5) Gibbs, H. M.; Khitrova, G.; Koch, S. W. Exciton-Polariton Light-Semiconductor Coupling Effects. *Nat. Photonics* **2011**, *5*, 273.

(6) Lodahl, P.; Mahmoodian, S.; Stobbe, S. Interfacing Single Photons and Single Quantum Dots with Photonic Nanostructures. *Rev. Mod. Phys.* **2015**, *87*, 347−400.

(7) Ribeiro, R. F.; Martínez-Martínez, L. A.; Du, M.; Campos-Gonzalez-Angulo, J.; Yuen-Zhou, J. Polariton Chemistry: Controlling Molecular Dynamics with Optical Cavities. *Chem. Sci.* **2018**, *9*, 6325−6339.

(8) Weisskopf, V. F.; Wigner, E. P. Calculation of the Natural Brightness of Spectral Lines on the Basis of Dirac's Theory. *Eur. Phys. J. A* **1930**, *63*, 54−73.

(9) Meystre, P. Theoretical Developments in Cavity Quantum Optics: a Brief Review. *Phys. Rep.* **1992**, *219*, 243−262.

(10) Meystre, P.; Sargent, M. *Elements of Quantum Optics*, 4th ed.; Springer Science & Business Media: New York, 2007.

(11) Thakkar, N.; Cherqui, C.; Masiello, D. J. Quantum Beats from Entangled Localized Surface Plasmons. *ACS Photonics* **2015**, *2*, 157−164.

(12) Power, E. A.; Thirunamachandran, T. Quantum Electrodynamics with Nonrelativistic Sources. I. Transformation to the Multipolar Formalism for Second-Quantized Electron and Maxwell Interacting Fields. *Phys. Rev. A.* **1983**, *28*, 2649−2662.

(13) Mukamel, S. *Principles of Nonlinear Optical Spectroscopy*; Oxford University Press: New York, 1999; pp 84−92.

(14) Note that obviously $[\hat{\mathbf{D}}_{\perp}, \hat{\mathcal{P}}_{\perp}] = 0$.

(15) Cohen-Tannoudji, C.; Dupont-Roc, J.; Grynberg, G. *Photons and Atoms: Introduction to Quantum Electrodynamics*; 1997.

(16) A straightforward proof of eq 4 is given here. Starting from eq 3

$$\hat{V}_{\mathrm{Coul}}^{(nl)} = \frac{1}{\epsilon_0}\int \mathrm{d}\mathbf{r}\, \hat{\boldsymbol{\mathcal{P}}}_{\parallel}^{(n)}(\mathbf{r})\cdot\hat{\boldsymbol{\mathcal{P}}}_{\parallel}^{(l)}(\mathbf{r}) = -\frac{1}{\epsilon_0}\int \mathrm{d}\mathbf{r}\, \hat{\boldsymbol{\mathcal{P}}}_{\perp}^{(n)}(\mathbf{r})\cdot\hat{\boldsymbol{\mathcal{P}}}_{\perp}^{(l)}(\mathbf{r}) = -\frac{1}{\epsilon_0}\int \mathrm{d}\mathbf{r}\, \hat{\boldsymbol{\mathcal{P}}}_{\perp}^{(n)}(\mathbf{r})\cdot\hat{\boldsymbol{\mathcal{P}}}^{(l)}(\mathbf{r})$$

Applying the definition of the transverse δ-function,

$$\hat{V}_{\mathrm{Coul}}^{(nl)} = -\frac{1}{\epsilon_0}\iint \mathrm{d}\mathbf{r}\,\mathrm{d}\mathbf{r}' \sum_{ij} \boldsymbol{\mu}_i\boldsymbol{\mu}_j \delta(\mathbf{r}-\mathbf{r}^{(n)})\delta_{\perp ij}(\mathbf{r}-\mathbf{r}')\delta(\mathbf{r}'-\mathbf{r}^{(l)}) = -\frac{1}{\epsilon_0}\iint \mathrm{d}\mathbf{r}\,\mathrm{d}\mathbf{r}' \sum_{ij} \boldsymbol{\mu}_i\boldsymbol{\mu}_j \delta(\mathbf{r}-\mathbf{r}^{(n)}) \times$$

$$\left[\frac{2}{3}\delta_{ij}\delta(\mathbf{r}-\mathbf{r}') + \frac{1}{4\pi|\mathbf{r}-\mathbf{r}'|^3}\left(\frac{3(\mathbf{r}_i-\mathbf{r}_i')(\mathbf{r}_j-\mathbf{r}_j')}{|\mathbf{r}-\mathbf{r}'|^2} - \delta_{ij}\right)\right]\delta(\mathbf{r}'-\mathbf{r}_{(l)})$$

Equation 4 is derived by evaluating the above double integral.

(17) Masiello, D.; Deumens, E.; Öhrn, Y. Dynamics of an Atomic Electron and Its Electromagnetic Field in a Cavity. *Phys. Rev. A.* **2005**, *71*, 032108.

(18) Lopata, K.; Neuhauser, D. Nonlinear Nanopolaritonics: Finite-Difference Time-Domain Maxwell-Schrödinger Simulation of Molecule-Assisted Plasmon Transfer. *J. Chem. Phys.* **2009**, *131*, 014701.

(19) Sukharev, M.; Nitzan, A. Numerical Studies of the Interaction of an Atomic Sample with the Electromagnetic Field in two Dimensions. *Phys. Rev. A.* **2011**, *84*, 043802.

(20) Puthumpally-Joseph, R.; Atabek, O.; Sukharev, M.; Charron, E. Theoretical Analysis of Dipole-Induced Electromagnetic Transparency. *Phys. Rev. A.* **2015**, *91*, 043835.

(21) Li, T. E.; Nitzan, A.; Sukharev, M.; Martinez, T.; Chen, H.-T.; Subotnik, J. E. Mixed Quantum-Classical Electrodynamics: Understanding Spontaneous Decay and Zero-Point Energy. *Phys. Rev. A.* **2018**, *97*, 032105.

(22) Prezhdo, O. V.; Rossky, P. J. Mean-Field Molecular Dynamics with Surface Hopping. *J. Chem. Phys.* **1997**, *107*, 825−834.

(23) Li, X.; Tully, J. C.; Schlegel, H. B.; Frisch, M. J. Ab Initio Ehrenfest Dynamics. *J. Chem. Phys.* **2005**, *123*, 084106.

(24) Parandekar, P. V.; Tully, J. C. Detailed Balance in Ehrenfest Mixed Quantum-Classical Dynamics. *J. Chem. Theory Comput.* **2006**, *2*, 229−235.

(25) Cotton, S. J.; Miller, W. H. Symmetrical Windowing for Quantum States in Quasi-Classical Trajectory Simulations. *J. Phys. Chem. A* **2013**, *117*, 7190−7194.

(26) Cotton, S. J.; Igumenshchev, K.; Miller, W. H. Symmetrical Windowing for Quantum States in Quasi-Classical Trajectory Simulations: Application to Electron Transfer. *J. Chem. Phys.* **2014**, *141*, 084104.

(27) West, B. J.; Lindenberg, K. Energy Transfer in Condensed Media. I. Two-Level Systems. *J. Chem. Phys.* **1985**, *83*, 4118−4135.

(28) Spano, F. C.; Mukamel, S. Superradiance in Molecular Aggregates. *J. Chem. Phys.* **1989**, *91*, 683−700.

(29) Alfonso Hernandez, L.; Nelson, T.; Tretiak, S.; Fernandez-Alberti, S. Photoexcited Energy Transfer in a Weakly Coupled Dimer. *J. Phys. Chem. B* **2015**, *119*, 7242−7252.

(30) Mirkovic, T.; Ostroumov, E. E.; Anna, J. M.; van Grondelle, R.; Govindjee; Scholes, G. D. Light Absorption and Energy Transfer in the Antenna Complexes of Photosynthetic Organisms. *Chem. Rev.* **2017**, *117*, 249−293.

(31) Andrews, D. L.; Juzeliunas, G. Intermolecular Energy Transfer: Retardation Effects. *J. Chem. Phys.* **1992**, *96*, 6606−6612.

(32) Andrews, D. L.; Craig, D. P.; Thirunamachandran, T. Molecular Quantum Electrodynamics in Chemical Physics. *Int. Rev. Phys. Chem.* **1989**, *8*, 339−383.

(33) Andrews, D. A Unified Theory of Radiative and Radiationless Molecular Energy Transfer. *Chem. Phys.* **1989**, *135*, 195−201.

(34) Scholes, G. D. Long-range Resonance Energy Transfer in Molecular Systems. *Annu. Rev. Phys. Chem.* **2003**, *54*, 57−87.

(35) Lakowicz, J. R. *Principles of Fluorescence Spectroscopy*; Springer Verlag: New York, 2006.

(36) Nelson, T.; Fernandez-Alberti, S.; Roitberg, A. E.; Tretiak, S. Conformational Disorder in Energy Transfer: Beyond Förster Theory. *Phys. Chem. Chem. Phys.* **2013**, *15*, 9245.

(37) Power, E. A.; Thirunamachandran, T. Quantum Electrodynamics with Nonrelativistic Sources. III. Intermolecular Interactions. *Phys. Rev. A.* **1983**, *28*, 2671−2675.

(38) Salam, A. *Molecular Quantum Electrodynamics: Long-Range Intermolecular Interactions*; John Wiley & Sons, 2010.

(39) This factor of 2 can be easily explained in the context of eq 21, given that we start with initial population 0.5 in the ground state for the donor.

(40) Schwabl, F. *Quantum Mechanics*, 4th ed.; Springer-Verlag: Berlin, 2007; p 306.

(41) Miller, W. H. A. Classical/Semiclassical Theory for the Interaction of Infrared Radiation with Molecular Systems. *J. Chem. Phys.* **1978**, *69*, 2188−2195.

(42) Mollow, B. R. Power Spectrum of Light Scattered by Two-Level Systems. *Phys. Rev.* **1969**, *188*, 1969−1975.

(43) Chen, H.-T.; Li, T. E.; Sukharev, M.; Nitzan, A.; Subotnik, J. E. Ehrenfest+R Dynamics I: A Mixed Quantum-Classical Electrodynamics Simulation of Spontaneous Emission. arXiv:1806.04662. http://arxiv.org/abs/1806.04662 (accessed Jun 12, 2018).

DOI: 10.1021/acs.jpclett.8b02309
J. Phys. Chem. Lett. 2018, 9, 5955−5961